UNIVERSITY OF AMSTERDAM

UvA-DARE (Digital Academic Repository)

Vibrational spectra of 1,3,5-hexatriene and methylated derivatives II. The coupling pattern for lateral methylation

Langkilde, F.W.; Amstrup, B.; Wilbrandt, R.; Brouwer, A.M.

Published in:
Spectrochimica acta. Part A. Molecular spectroscopy

Link to publication

Citation for published version (APA):
Langkilde, F. W., Amstrup, B., Wilbrandt, R., & Brouwer, A. M. (1989). Vibrational spectra of 1,3,5-hexatriene and methylated derivatives II. The coupling pattern for lateral methylation. Spectrochimica acta. Part A. Molecular spectroscopy, 45A, 883-903.

General rights
It is not permitted to download or to forward/distribute the text or part of it without the consent of the author(s) and/or copyright holder(s), other than for strictly personal, individual use, unless the work is under an open content license (like Creative Commons).

Disclaimer/Complaints regulations
If you believe that digital publication of certain material infringes any of your rights or (privacy) interests, please let the Library know, stating your reasons. In case of a legitimate complaint, the Library will make the material inaccessible and/or remove it from the website. Please Ask the Library: http://uba.uva.nl/en/contact, or a letter to: Library of the University of Amsterdam, Secretariat, Singel 425, 1012 WP Amsterdam, The Netherlands. You will be contacted as soon as possible.

UvA-DARE is a service provided by the library of the University of Amsterdam (http://dare.uva.nl)

Download date: 24 Feb 2017

Spectrochimica Acta, Vol. 45A, No. 9, pp. 883–903, 1989.
Printed in Great Britain.

0584–8539/89 $3.00+0.00
© 1989 Pergamon Press plc

Vibrational spectra of 1,3,5-hexatriene and methylated derivatives—II. The coupling pattern for lateral methylation

FRANS W. LANGKILDE,*† BJARNE AMSTRUP,* ROBERT WILBRANDT* and ALBERT M. BROUWER‡§

*Chemistry Department, Risø National Laboratory, DK-4000 Roskilde, Denmark; and ‡Gorlaeus Laboratories, State University at Leiden, NL-2300 RA Leiden, The Netherlands

(*Received* 1 *December* 1988; *in final form* 26 *January* 1989; *accepted* 27 *January* 1989)

Abstract—The vibrational spectra of *E*-2-methyl-hexatriene (E2MH), 4-*d*-*E*-2-methyl-hexatriene (dE2MH), and *E*-3-methyl-hexatriene (E3MH) were measured and interpreted using semi-empirical QCFF/π calculations and empirical valence force field (VFF) calculations. The vibrational patterns of E2MH and E3MH are discussed on the basis of the VFF calculations. It is found that the vibrational pattern of E3MH resembles that of *E*-1,3,5-hexatriene whose normal modes to a high degree can be described by global symmetry coordinates, whereas the pattern of E2MH resembles that of isoprene whose normal modes are more influenced by local symmetry coordinates. The effect of steric hindrance on methyl group conformation and the coupling of the methyl group vibrations with those of the polyene chain are discussed.

INTRODUCTION

Vibrational analysis of 1,3,5-hexatrienes has been reported by many authors [1–21]. We have been interested in the vibrations of hexatrienes in both the ground state [1] and the lowest excited triplet state, detected by time-resolved resonance Raman spectroscopy [22–27].

Since our first study of hexatriene ground state vibrations, four papers have appeared that analyze these vibrations by semi-empirical [13] and scaled *ab initio* [9, 20, 21] methods. These calculations support our vibrational analysis of hexatriene. One reason for the authors of these papers to study hexatriene vibrations is that hexatriene is a model for polyacetylene, the infinite length conducting polyene. With the growth in polyacetylene studies [28], it is important to understand the hexatriene vibrations, and to determine the properties that influence them.

In [1] we studied the Raman and i.r. spectra of the ground state of *E*-1,3,5-hexatriene and derivatives that were methylated in the terminal position: *E*,*E*-1,3,5-heptatriene and *E*,*E*,*E*-2,4,6-octatriene, or in lateral positions: *E*-2,5-dimethyl-1,3,5-hexatriene. The strongest effect observed in this study was seen upon lateral methylation. For *E*-2,5-dimethyl-1,3,5-hexatriene, the stretching vibrations of the C–C single bonds of the polyene chain and of the C–C single bonds between the chain and the methyl groups were strongly coupled. As a consequence, the C–C single bond stretching vibrations were split into high-wavenumber out-of-phase combinations and low-wavenumber in-phase combinations.

To investigate this effect further, we here study the two hexatrienes that are substituted laterally with only one methyl group: *E*-2-methyl-1,3,5-hexatriene (E2MH) and *E*-3-methyl-1,3,5-hexatriene (E3MH), because in this case it is possible to distinguish between the isolated C–C single bond and the methylated C–C single bond of the polyene chain. Moreover, as it turns out below, the influence of the lateral methyl group on the vibrational pattern is dependent upon whether the methyl group is in the 2- or the 3-position. Here, hexatriene is more interesting to study than butadiene, since it has two *different* lateral positions.

Scheme 1

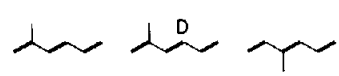

Consequently, from a vibrational analysis of E2MH and E3MH, we expect to gain information on the coupling between vibrations. As vibrations, through the force constants or force field, express the potential energy in chemical bonds, this study should further lead to increased insight into the interaction between chemical bonds.

In the present paper we report the Raman and Fourier transform (FT) i.r. spectra of *E*-2-methyl-hexatriene and *E*-3-methyl-hexatriene. To support the vibrational analysis, we also obtained the Raman spectrum of one deuterated derivative: 4-*d*-*E*-2-methyl-hexatriene (dE2MH).

The experimental spectra are interpreted by calculation, using two kinds of force fields: (1) An empirical valence force field, based on literature values for

†To whom correspondence should be addressed.
§Present address: Laboratory of Organic Chemistry, University of Amsterdam, NL-1018, WS Amsterdam, The Netherlands.

butadiene, isoprene, and *E*-1,3,5-hexatriene and refined in the present study, and (2) a valence force field computed by the semi-empirical QCFF/π program. The coupling patterns are discussed on the basis of the calculated internal coordinate contributions to the normal modes.

EXPERIMENTAL

The synthesis of E2MH, dE2MH, and E3MH has been described in detail previously [29]. Analytical GC (BP10 capillary column, 62°C) of E2MH showed no detectable impurities, whereas the E3MH sample was found to contain 97% *E*-3-methyl-hexatriene, 1% *Z*-3-methyl-hexatriene and 2% 2-methyl-1,3-cyclohexadiene.

The samples were captured in capillary glass tubes in a cold trap under reduced pressure (~0.1 mmHg). The capillaries were sealed and kept in a freezer. The Raman spectra were obtained from samples in capillary glass tubes (outer diameter 3 mm), thermostatted at 15°C (22°C for dE2MH). The FT-i.r. spectrum of matrix-isolated E2MH was obtained from a 1:300 sample in argon at 15 K. E3MH was transferred under argon to a vacuum line, dried over P_2O_5, and transferred to a spectroscopic cell for the gas phase FT-i.r. spectrum. This spectrum was recorded at room temperature at pressures from 6 to 13 mmHg.

The Raman spectra in the region 2000–10 cm^{-1} were recorded with a DILOR Z24 triple monochromator equipped with a cooled Centronix P4283 PM-tube. The exciting source was the green 514.5 nm line from a Spectra-Physics model 165 argon-ion laser with an output of 400 mW. The vertically polarized laser light was passed through a monochromator to remove laser lines other than the 514.5 nm one, reducing the laser power to 170 mW. Perpendicular illumination was used in a horizontal scattering plane. Spectra were obtained in I_{VV} and I_{VH} configurations. A quarter-wave plate was placed in front of the monochromator entrance slit to ensure circularly polarized light. The spectral slit width was 2.9 cm^{-1} or less, the registration speed was 60 cm^{-1} per min, and the step in frequency was 1 cm^{-1}.

The FT-i.r. spectrum of gas phase E3MH was recorded on a Bruker IFS 113v spectrometer equipped with an Aspect 3000 computer. Mid i.r. spectra were obtained in the region 4000–550 cm^{-1} with a resolution of 0.5 cm^{-1}. A Ge/KBr beam splitter and a liquid nitrogen cooled MCT detector with KBr windows were used. Far i.r. spectra were obtained in the region 700–300 cm^{-1} with 1 cm^{-1} resolution using a room temperature DTGS detector with polyethylene windows. The spectroscopic cell was a 10 cm gas cell with KBr windows.

The FT-i.r. spectrum of matrix-isolated E2MH was recorded on a Digilab FTS 15 spectrometer in the region 4000–400 cm^{-1} with 2 cm^{-1} resolution [30]. In these experiments a mixture of E2MH and Ar (1:300) was deposited on an aluminum mirror [31]. KBr windows and a TGS detector were used.

We used two different approaches for the force field calculations, one with an empirical valence force field from the literature which was subsequently refined, the other with a semi-empirical quantum chemical force field.

In the first approach, one program, VIBROT [32], calculates the wavenumbers and internal coordinate composition of the normal modes from the molecular geometry, the internal coordinates, the nuclear masses, and the valence force field. The valence force field is refined using another program, FLINDA [32]. Here, the input consists of the molecular geometry, the internal coordinates, the nuclear masses, the experimentally observed frequencies, and starting values for the valence force field. For each force constant it is specified whether it should be kept fixed or varied in the refinement. Both the fixed and variable force constants are divided into sets, where all the force constants in a set must have the same value. By least-squares analysis, FLINDA iterates a new force field.

In the second approach, the QCFF/π program [33] was obtained from QCPE in an IBM version [34].

The VIBROT and FLINDA calculations were implemented on an RC8000 computer at the H.C. Ørsted Institute, Copenhagen University, and the QCFF/π calculations were

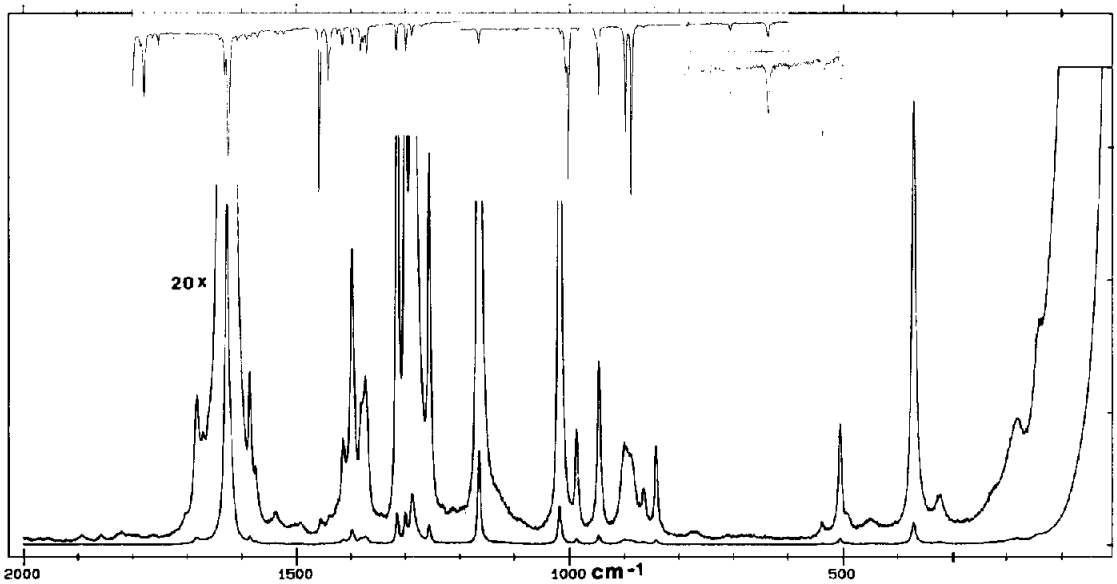

Fig. 1. Top: FT-i.r. spectrum of 1:300 *E*-2-methyl-hexatriene in argon matrix at 15 K. Linear in per cent transmission, the relative scales are 1.5:3.5:1 in the regions 1800–1200, 1200–600 and 800–500 cm^{-1} respectively. Resolution 2 cm^{-1}, windows KBr, detector TGS. Bottom: Raman spectrum of neat *E*-2-methyl-hexatriene at 15°C, I_{vv} configuration.

carried out at the computer centre at Leiden. In the following, the VIBROT and FLINDA programs shall be referred to as VFF, and the QCFF/π as QCFF.

RESULTS

The FT-i.r. spectrum of matrix-isolated *E*-2-methyl-hexatriene and the Raman spectrum of the neat compound are shown in Fig. 1. The wavenumbers and intensities of the observed bands are listed in Table 1, together with the Raman depolarization ratios. Also listed are calculated wavenumbers and i.r. intensities. The Raman spectrum of neat 4-*d*-*E*-2-methyl-hexatriene is shown in Fig. 2. Wavenumbers, intensities and Raman depolarization ratios are listed in Table 2, together with calculated wavenumbers. The FT-i.r. spectrum of gas phase *E*-3-methyl-hexatriene and the Raman spectrum of the neat compound are shown in Fig. 3. Wavenumbers, intensities, Raman depolarization ratios and i.r. band contours are listed in Table 3, together with calculated wavenumbers and i.r. intensities.

The Raman bands in the low frequency region are obscured by the strong Rayleigh line. An established method [35] to remove the Rayleigh line is to replace the Raman spectrum with the $R(\bar{\nu})$ spectrum. $R(\bar{\nu})$ is defined as

$$\bar{\nu}[1-\exp(-h\bar{\nu}c/kT)]I(\bar{\nu}),$$

where $\bar{\nu}$ is the Raman shift in cm^{-1}, h is Planck's constant, k is Boltzmann's constant, T is the absolute temperature, and c is the velocity of light.

The $R(\bar{\nu})$ spectra in the region below 400 cm^{-1} are shown in Figs 4A–4C for E2MH, dE2MH and E3MH, respectively. The Raman wavenumbers, intensities and depolarization ratios listed in Tables 1–3 for bands below 400 cm^{-1} were obtained from the $R(\bar{\nu})$ spectra.

The atom numbering, internal coordinates and bond lengths and angles used for E2MH, dE2MH and E3MH are shown in Fig. 5. To compensate for anharmonicity, we used spectroscopic masses [36, 37]. The results of the VFF calculations are shown in Tables 4–6 for E2MH, dE2MH and E3MH, respectively. The calculated wavenumber and potential energy distribution of each normal mode are listed. The potential energy distributions are normalized. They

Table 1. Observed wavenumbers (cm^{-1}) and depolarization ratios of Raman bands and wavenumbers of i.r. bands of *E*-2-methyl-hexatriene in the region 2000–10 cm^{-1}, together with approximate assignments and calculated wavenumbers and i.r. intensities

Raman (liquid)	I_{VH}/I_{VV}	Infrared (matrix)	Assignment	VFF wavenumber	QCFF wavenumber	QCFF intensity
1893 w	0.23					
1859 w	0.23					
1820 w	0.22					
		1798 m				
		1785 w				
		1778 m				
		1776 sh				
1762 w	0.39	1763 w				
		1752 w				
1702 sh	0.43					
1682 m	0.25					
1670 w	0.34					
		1640 w				
		1631 m	νC=C	1644	1678	0.13
1627 s	0.21	1623 s	νC=C	1626	1653	0.20
		1608 w				
		1591 w				
1585 m	p		νC=C	1574	1600	0.02
1575 w	p	1571 w				
1538 w	0.25	1534 w				
		1523 w				
1494 w	0.23					
1455 w	0.50	1457 s	dCH$_3$	1453	1469	1.49
1440 w	0.75	1442 m	dCH$_3$	1449	1475	0.78
		1437 sh				
1426 sh		1424 w				
1415 m	0.34	1415 w	sCH$_2$	1428	1457	1.43
1398 m	0.23	1397 w	sCH$_2$	1403	1435	0.75
1381 sh	0.37	1383 m				
		1378 w				
1374 m	0.32	1371 m	dCH$_3$	1381	1444	2.22
1316 s	0.30	1317 m	νC–C	1320	1408	0.10
1301 s	0.22	1299 m	rCH	1287	1350	0.05
1288 s	0.21	1288 w	rCH	1284	1318	2.29
		1270 w				

Table 1. (*continued*)

Raman (liquid)	I_{VH}/I_{VV}	Infrared (matrix)	Assignment	VFF wavenumber	QCFF wavenumber	QCFF intensity
1257 m	0.26		*r*CH	1251	1293	0.57
1213 w	p					
		1167 sh				
1166 s	0.30	1166 m	*v*C–C	1162	1196	1.10
		1040 w	*w*CH_3	1038	1060	2.44
1019 s	0.23	1016 w	*r*CH_3	1008	1026	0.81
		1007 m				
		1002 s	*w*CH	1002	1072	1.24
988 m	0.25	986 w	*r*CH_2	985	982	0.29
		953 sh				
		950 sh				
947 m	0.37	947 s	*r*CH_2	949	948	0.83
900 m	0.70	898 s	*w*CH	910	1001	1.28
894 sh	0.70		*w*CH_2	908	952	0.43
888 m	0.69	887 s	*w*CH_2	897	950	2.82
		880 w				
865 m	0.68	865 w	*w*CH	870	864	0.02
843 m	0.42		*v*C–C	829	921	0.07
773 w	0.56					
705 w	0.70	707 w	*t*C=C	707	732	0
684 w	0.36					
634 w	0.74	638 w	*t*C=C	633	629	0.62
540 w	0.59	538 m	*d*CCC	549	606	0.15
507 m	0.13	505 w	*d*CCC	513	562	0.43
493 w	0.75		*w*CH_3	484	476	0.59
452 w	0.40					
372 s	0.32		*d*CCC	358	395	0
325 m	0.63		*d*CCC	330	374	0.11
			*t*C–C	309	227	0.13
229 w			*rot*CH_3	202	202	0.01
186 m	0.74		*t*C=C	174	162	0.19
			*d*CCC	134	166	0.14
146 w	0.73		*t*C – C	114	91	0.04
55 m	0.76		inter-molecular			

s = strong, m = medium, w = weak, sh = shoulder; p = polarized, dp = depolarized; *v* = stretch, *d* = deformation, *s* = scissoring, *r* = in-plane rock, *w* = out-of-plane wag, *t* = twist, *rot* = rotation.

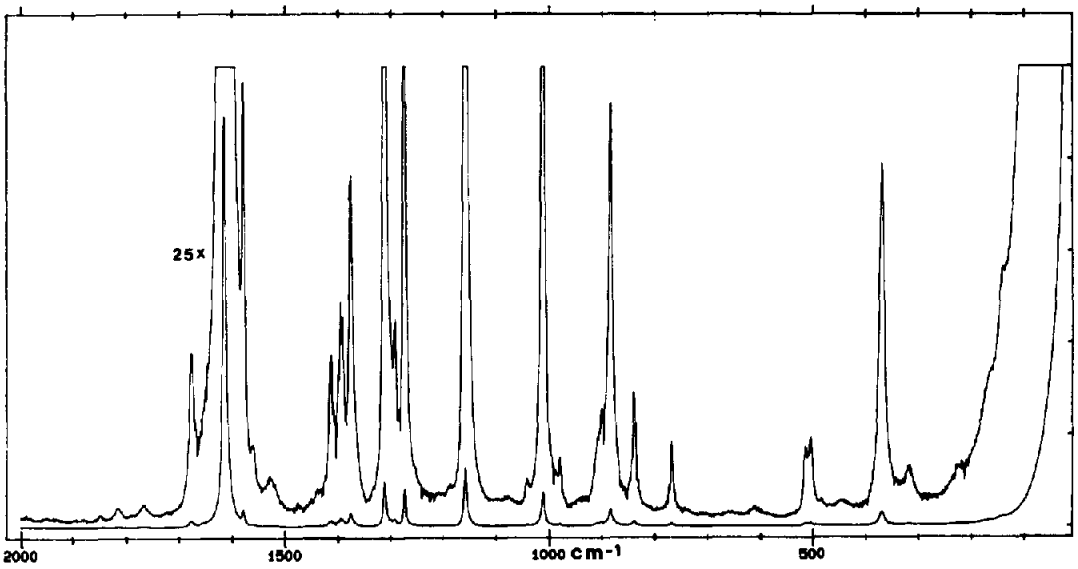

Fig. 2. Raman spectrum of neat 4-*d*-*E*-2-methyl-hexatriene at 22°C, I_{vv} configuration.

Table 2. Observed wavenumbers (cm^{-1}) and depolarization ratios of Raman bands of 4-*d*-*E*-2-methyl-hexatriene in the region 2000–10 cm^{-1}, together with approximate assignments and calculated wavenumbers

Raman (liquid)	I_{VH}/I_{VH}	Assignment	VFF wavenumber	QCFF wavenumber
1848 w	p			
1816 w	0.28			
1766 w	0.30			
1677 m	0.25			
1628 sh		*v*C=C	1644	1674
1615 s	0.20	*v*C=C	1620	1646
1578 m	0.42	*v*C=C	1563	1592
1561 w	0.50			
1528 w	0.24			
1475 w	p			
1450 w	0.47	*d*CH_3	1453	1468
1439 w	0.72	*d*CH_3	1449	1475
1424 sh	p			
1413 m	0.35	*s*CH_2	1426	1454
1393 m	0.31	*s*CH_2	1403	1434
1376 m	0.36	*d*CH_3	1381	1444
1311 s	0.28	*v*C–C	1314	1406
1292 m	0.19	*r*CH	1286	1330
1274 s	0.19	*r*CH	1268	1298
1188 w	p			
1159 s	0.38	*v*C–C	1159	1197
		wCH_3	1036	1061
1039 w	0.33	*r*CD/*r*CH_2	1029	1049
1011 s	0.26	*r*CH_3	996	1021
992 w	dp	*w*CH	1000	1052
980 w	0.44	*r*CH_2	985	981
907 sh	dp	*w*CH_2	909	953
900 m	dp	*w*CH	899	937
897 sh	dp	*w*CH_2	897	950
884 m	0.33	*r*CD/*r*CH_2	890	895
839 m	0.71	*v*C–C	829	922
768 m	0.77	*w*CD	740	771
743 w				
707 w	0.75	*t*C=C	707	727
657 w	0.33			
612 w	0.77	*t*C=C	611	615
515 m	0.26	*d*CCC	530	588
506 m	0.13	*d*CCC	512	558
485 w	0.79	*w*CH_3	478	473
446 w	0.45			
370 m	0.39	*d*CCC	358	394
320 w	0.63	*d*CCC	326	370
		*t*C–C	296	226
278 w				
225 w	dp	*rot*CH_3	201	199
169 w	dp	*t*C=C	166	151
		*d*CCC	134	165
143 w	dp	*t*C–C	114	90
49 m	dp	inter-molecular		

are calculated as the square of the coefficient of an internal coordinate in a normal mode, multiplied by the pertinent diagonal force constant. However, the sign of the coefficients is retained in the potential energy distribution. Only the dominant contributions are shown; in most cases these are the internal coordinates that contribute more than 10% to the normal mode. The valence force field applied to E2MH and dE2MH is listed in Table 7, the one applied to E3MH in Table 8.

DISCUSSION

Empirical valence force fields

The valence force field in Table 7 for *E*-2-methyl-hexatriene and 4-*d*-*E*-2-methyl-hexatriene was constructed on the basis of force fields for butadiene, isoprene and *E*-hexatriene. These three latter force fields were again based on values from Ref. [15] (CT). In CT, force constants derived from smaller molecules are used to construct the force fields of retinals. This

Table 3. Observed wavenumbers (cm^{-1}) and depolarization ratios of Raman bands and wavenumbers and band contours of infrared bands of E-3-methylhexatriene in the region 2000–10 cm^{-1}, together with approximate assignments and calculated wavenumbers and infrared intensities

Raman (liquid)	I_{VH}/I_{VV}	R	Infrared (gas) Q	P	Contour	Assignment	VFF wavenumber	QCFF wavenumber	QCFF infrared intensity
1966 w	0.33		1964		w				
1891 w	0.35								
			1878		w				
1869 w	0.30								
1808 w	0.49	1819	1807	1798	m				
			1766		w				
1744 w	p								
1679 m	0.34								
1624 s	0.24	1628		1620	s *B*	νC=C	1637	1672	0.05
1620 sh	0.25	1624		1617	sh *B*	νC=C	1623	1646	0.19
1602 sh	0.25								
1577 m	p		1585		w	νC=C	1583	1600	0.05
1550 w	p		1544		w				
1532 w	0.30								
			1515		w				
1459 w	0.47					dCH$_3$	1453	1496	1.72
1443 w	0.56		1448		sh *C*	dCH$_3$	1449	1471	0.74
1424 m	0.41	1432	1428	1423	m *A*	sCH$_2$	1429	1446	2.10
1413 s	0.29								
1402 s	0.28					sCH$_2$	1400	1424	0.74
1387 sh	0.59	1395		1387	m *B*	dCH$_3$	1382	1440	2.96
1348 m	0.29	1355	1350	1345	w *A*	νC–C	1340	1479	0.51
1323 m	0.21		1319		w				
1298 s	0.19	1300	1295	1291	w. *A*	rCH	1286	1330	0.24
1257 m	0.31	1261		1253	w	rCH	1272	1312	0.08
1226 s	0.27	1230		1219	w	rCH	1223	1268	0.48
1155 sh	0.43		1154		sh				
1145 m	0.43		1144		m	νC–C	1142	1203	0.63
1106 w	0.43								
1067 s	0.32	1073	1069	1064	m *A*	rCH$_3$	1037	1067	1.37
1034 w	0.67		1034		w	wCH$_3$	1022	1055	0.34
			990		s *C*	wCH	996	1047	1.69

985 m	0.26						rCH$_2$	980	1019	0.36
			984		s	*C*	wCH	993	1036	0.64
946 w	0.18	952	947	942	w	*A*	rCH$_2$	936	939	0.31
906 m	0.69		906		s	*C*	wCH$_2$	908	956	0.85
901 m	0.73		899		s	*C*	wCH$_2$	906	954	4.18
843 w	0.70									
803 m	0.67		806		w		wCH	812	904	0.15
			788		w		vC–C	792	873	0.42
738 w	p	748		743	w					
			685		m	*C*	tC=C	687	657	0.01
			668		m	*C*	CO$_2$ *Q*-branch			
648 w	0.73		641		m	*C*	tC=C	655	642	1.01
584 w	0.63	588	583	579	w	*A*	dCCC	576	663	0.72
567 w	dp									
			550		w					
492 w	0.30									
456 w	0.06	458	454	448	w	*A*	dCCC	439	490	0.06
420 w	0.73		415		m	*C*	wCH$_3$	421	441	0.64
			399		m	*C*				
392 s	0.24	394	391	387	w		dCCC	360	425	0
337 w										
301 w							dCCC	291	372	0.09
256 w							tC=C	275	236	0.21
							tC–C	204	168	0
181 w	0.72						rotCH$_3$	194	126	0.01
							dCCC	158	208	0.20
156 w	0.75						tC–C	126	97	0.12
46 m	0.77						inter-molecular			

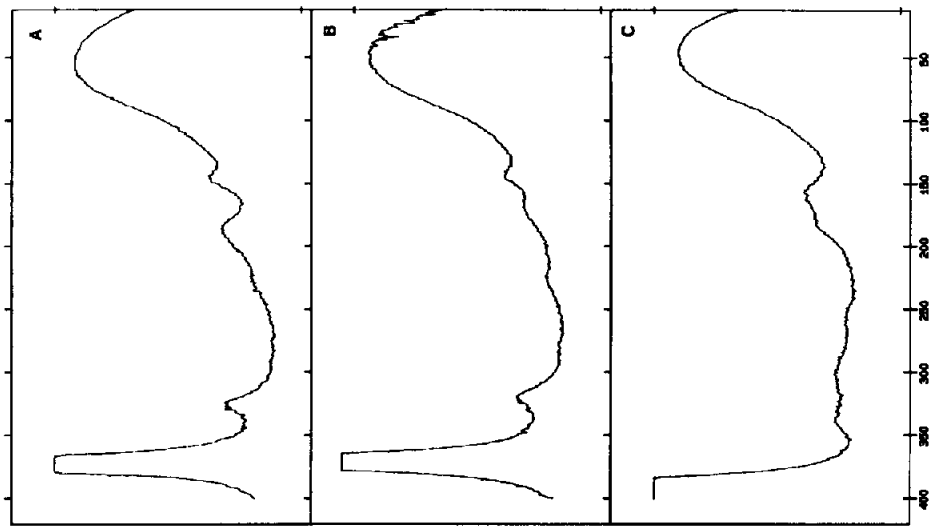

Fig. 4. Raman $R(\nu)$ spectra of neat *E*-2-methyl-hexatriene at 15°C (A), 4-*d*-*E*-2-methyl-hexatriene at 22°C (B), and *E*-3-methyl-hexatriene at 15°C (C), I_{vv} configuration.

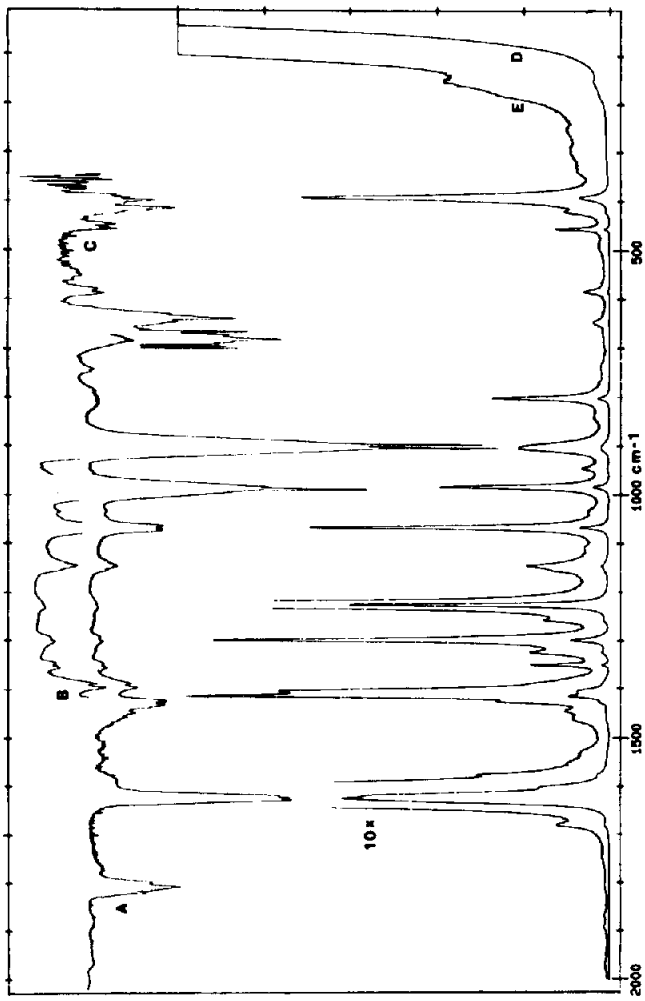

Fig. 3. (A–C): FT-i.r. spectrum of gas phase *E*-3-methyl-hexatriene at room temperature, pressure is ~6 mmHg (A) and ~13 mmHg (B, C). Linear in per cent transmission, the relative scales are 2.8 : 4.0 : 1 for (A), (B) and (C), respectively. Cell length 10 cm, windows KBr. Resolution 0.5 cm^{-1} (A, B) and 1.0 cm^{-1} (C) Detectors MCT with KBr windows (A, B) and DTGS with PE windows (C), beam splitter Ge/KBr. Cut-off in (C) at 700 cm^{-1} due to detector PE windows, at 350 cm^{-1} to cell KBr windows. (D) (E): Raman spectrum of neat *E*-3-methyl-hexatriene at 15°C, I_{vv} configuration.

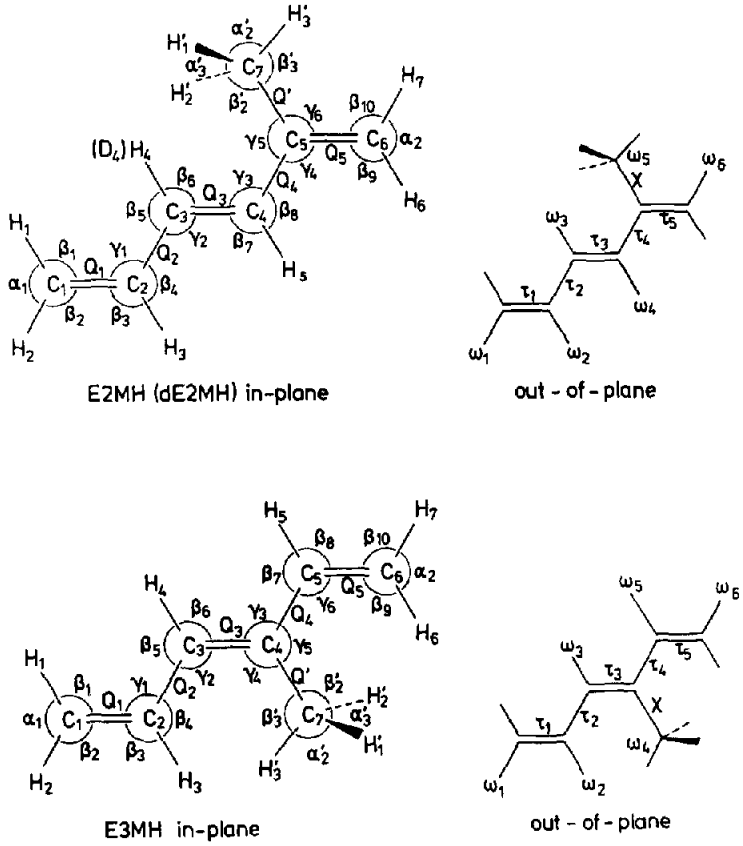

Fig. 5. Atom numbering and internal coordinates of *E*-2-methyl-hexatriene (E2MH) and *E*-3-methyl-hexatriene (E3MH). CH stretches, q_i and q'_j, are numbered according to the hydrogen atoms involved. Q CC stretch, α HCH scissoring, β CCH rock, γ CCC bend. ω CH or C–CH_3 out-of-plane wag, towards the reader. τ_1 $H_2C_1C_2C_3$ torsion, H_2 and C_3 towards the reader. τ_2 $C_1C_2C_3C_4$ torsion, C_1 and C_4 away from the reader. $\tau_3C_2C_3C_4C_5$ torsion, $\tau_4C_3C_4C_5C_6$ torsion, $\tau_5C_4C_5C_6H_7$ torsion. For E2MH: χ $C_4C_5C_7H'_1 + C_4C_5C_7H'_2 + C_4C_5C_7H'_3$ torsions, with C_4 and H'_3 away from the reader. For E3MH: χ $C_5C_4C_7H'_1 + C_5C_4C_7H'_2 + C_5C_4C_7H'_3$ torsions, with C_5 and H'_3 away from the reader. Geometrical parameters are $q_1 - q_7 = 1.084$ Å, $Q_1 = Q_5 = 1.337$ Å, $Q_2 = Q_4 = 1.458$ Å, $Q_3 = 1.368$ Å, $Q' = 1.52$ Å, $\beta_1 = \beta_2 = \beta_9 = \beta_{10} = 120.5°$, $\beta_3 = \beta_4 = 119.15°$, $\beta_5 = \beta_6 = \beta_7 = \beta_8 = 117.8°$, $\alpha_1 = \alpha_2 = 119°$, $q' = 1.105$ Å, $\alpha' = \beta' = 109.47°$. For E2MH, $\gamma_1 = 121.7°$, $\gamma_2 = \gamma_3 = 124.4°$, $\gamma_4 = 123.2°$, $\gamma_5 = \gamma_6 = 118.4°$. For E3MH, $\gamma_1 = 121.7°$, $\gamma_2 = \gamma_6 = 124.4°$, $\gamma_3 = 123.2°$, $\gamma_4 = \gamma_5 = 118.4°$. Atom numbering, internal coordinates, and geometrical parameters are identical for E2MH and dE2MH. Spectroscopic masses were used: $m_H = 1.088$, $m_D = 2.126$, $m_C = 12.0$.

work is probably the most thorough study of polyene vibrations; it is described at length in Ref. [38].

Since the butadiene force field in CT is iterated on the basis of observed vibrational spectra of as many as eleven different isotopic derivatives of butadiene, we used the CT butadiene force constants as the starting point in our iteration. Also the molecular geometry, i.e. bond lengths and angles, used in the present study, was transferred from CT, apart from the conformation of the methyl groups (see below). The molecular geometry in CT is closely related to the experimentally found one [39].

To model the effect of methylation, we constructed an isoprene valence force field after values from CT for propene and isoprene. For these compounds a good agreement is found in CT between calculated and observed vibrational wavenumbers. A more recent study of isoprene [40] supports the CT isoprene values. CT mainly uses a modified Urey–Bradley force field [36, 41], whereas we use a valence type of force field. As seen from Table 7, we refined some of the isoprene force constants, using the VFF programs and experimental frequencies cited in CT (mostly from Ref. [42]).

The effect of elongation of the polyene chain going from butadiene to *E*-hexatriene, was only partly modelled after values from CT, since we disagree in the assignment of the *E*-hexatriene vibrations at 1288, 1283 and 1132 cm^{-1} (our values) [1, 15]. Compared to CT, we modified the in-plane force field for *E*-hexatriene. In our choice of starting values for the refinement we took into account the values used in two of the most recent calculations [9, 20].

The valence force fields obtained as described above for butadiene, isoprene and *E*-hexatriene, were used to

Table 4. Calculated wavenumbers (cm^{-1}) and potential energy distributions of the normal modes of *E*-2-methyl-hexatriene in the region below 2000 cm^{-1}. Only the dominant contributions are shown. For notation, see Fig. 5

Wavenumber	Potential energy distribution
1644	$0.54\ Q_5\ -0.10\ Q_4$
1626	$0.47\ Q_1\ -0.10\ Q_2\ +0.09\ Q_3$
1574	$0.45\ Q_3\ -0.10\ Q_1$
1453	$0.64\ \alpha'_3\ -0.14\ \alpha'_1\ -0.14\ \alpha'_2$
1449	$0.47\ \alpha'_1\ -0.47\ \alpha'_2$
1428	$0.21\ \alpha_1\ -0.10\ \beta_2\ -0.20\ \alpha_2\ +0.10,\ \beta_{10}$
1403	$0.19\ \alpha_1\ -0.09\ \beta_2\ +0.19\ \alpha_2\ -0.09\ \beta_{10}$
1381	$0.15\ \alpha'_1\ +0.15\ \alpha'_2\ +0.08\ \alpha'_3$
	$-0.14\ \beta'_1\ -0.14\ \beta'_2\ -0.14\ \beta'_3$
1320	$0.20\ Q'\ -0.14\ Q_4\ -0.06\ \beta_6\ -0.07\ \beta_9\ +0.06\ \gamma_3\ +0.08\ \gamma_4$
1287	$0.26\ \beta_3\ -0.18\ \beta_4\ +0.09\ \beta_1\ -0.09\ \beta_7\ +0.19\ Q_1$
1284	$0.19\ \beta_7\ -0.14\ \beta_8\ +0.06\ \beta_3\ +0.11\ Q_3\ +0.08\ Q'$
1251	$0.32\ \beta_5\ -0.28\ \beta_6\ +0.11\ \beta_7\ -0.11\ \beta_8$
1162	$0.40\ Q_2\ +0.13\ \beta_4$
1038	$0.31\ \beta'_1\ -0.31\ \beta'_2\ +0.12\ \omega_5\ -0.15\ \omega_6$
1008	$0.40\ \beta'_3\ -0.09\ \beta'_1\ -0.09\ \beta'_2\ +0.11\ Q_4$
1002	$0.79\ \omega_2\ -0.12\ \tau_1$
985	$0.27\ \beta_9\ -0.31\ \beta_{10}\ +0.14\ \beta'_3\ -0.08\ Q_4$
949	$0.29\ \beta_1\ -0.32\ \beta_2\ -0.19\ Q_2$
910	$0.31\ \omega_3\ -0.31\ \omega_4\ +0.16\ \tau_5$
908	$0.71\ \omega_1\ +0.25\ \tau_1$
897	$0.63\ \omega_6\ +0.10\ \omega_4\ +0.17\ \tau_5$
870	$0.43\ \omega_3\ +0.25\ \omega_4\ -0.11\ \omega_6$
829	$0.61\ Q'\ +0.16,\ Q_4$
707	$0.63\ \tau_5\ +0.11\ \tau_1$
633	$0.46\ \tau_1\ +0.32\ \omega_2$
549	$0.24\ \gamma_5\ -0.19\ \gamma_3\ +0.17\ \gamma_1\ -0.11\ \gamma_4$
513	$0.35\ \gamma_6\ +0.10\ \gamma_2\ -0.09\ \gamma_4$
484	$0.57\ \omega_5\ -0.10\ \tau_3\ +0.07\ \tau_5$
358	$0.21\ \gamma_1\ +0.19\ \gamma_4\ -0.12\ \gamma_6\ +0.09\ Q_2\ +0.08\ Q_3\ +0.10\ Q_4$
330	$0.21\ \gamma_5\ +0.18\ \gamma_2\ -0.14\ \gamma_1\ +0.11\ Q_4$
309	$0.40\ \tau_2\ -0.36\ \tau_4$
202	$0.76\ \chi$
174	$0.57\ \tau_3\ +0.09\ \omega_3\ +0.10\ \omega_4\ +0.12\ \omega_5$
134	$0.33\ \gamma_3\ -0.26\ \gamma_2\ +0.10\ \gamma_1$
114	$0.33\ \tau_3\ -0.18\ \tau_2\ -0.15\ \tau_4\ +0.15\ \omega_3\ +0.13\ \omega_4$

construct an initial force field in the iteration of the *E*-2-methyl-hexatriene force field, using the VFF programs; this refinement caused only a few changes as seen from Table 7. The *E*-2-methyl-hexatriene force field was transferred to *E*-3-methyl-hexatriene with only minor changes, see Table 8.

A proper discussion of the valence force fields in Tables 7 and 8 would be quite extensive. Here, we shall only give a brief comparison of our values with the scaled *ab initio* values from Refs [9, 20, 21].

Our diagonal force constants for the CC stretches of the chain, Q_1–Q_5, tend to be lower than those of the references mentioned. So are our values for the interaction between neighbouring chain CC stretches, whereas our values for the interaction between next-neighbour chain CC stretches, i.e. Q_1Q_3, Q_3Q_5 and Q_2Q_4, are (numerically) larger than in the references. Our diagonal force constants for the CH rocks are larger, those of the terminal CCC bends are smaller, and our value for the interaction between the two central CCC bends is larger than in the references mentioned.

Molecular geometry and vibrational band types

E-2-methyl-hexatriene has been found by the gas electron diffraction method to be planar with *tEt* geometry [39]. This result was confirmed for the liquid phase using u.v. absorption and NMR spectroscopy [29]. The latter study found *E*-3-methyl-hexatriene as well to be planar with *tEt* geometry. Consequently, both molecules transform according to C_s symmetry, and all 45 normal modes of vibration are in principle both Raman and i.r. active. Thirty in-plane modes of a' symmetry have polarized Raman bands and *A*, *B*, or *A*/*B* hybrid type gas phase i.r. bands, whereas 15 a'' out-of-plane modes have depolarized Raman bands and *C* type gas phase i.r. bands. Among the 45 modes of vibration, 10 are CH stretch fundamentals around 3000 cm^{-1}. These shall not be dealt with in the present study; out of these, nine are in-plane (a') and one is out-of-plane (a'').

The question of the conformation of the methyl group must be addressed separately. If one methyl hydrogen is assumed to be in the plane of the molecu-

Table 5. Calculated wavenumbers (cm^{-1}) and potential energy distributions of the normal modes of 4-*d*-*E*-2-methyl hexatriene in the region below 2000 cm^{-1}. Only the dominant contributions are shown. For notation, see Fig. 5

Wavenumber	Potential energy distribution
1664	$0.56\ Q_5\ -0.09\ Q_4$
1620	$0.52\ Q_1\ -0.09\ Q_2\ +0.10\ \alpha_1$
1563	$0.53\ Q_3$
1453	$0.64\ \alpha'_3\ -0.14\ \alpha'_1\ -0.14\ \alpha'_2$
1449	$0.47\ \alpha'_1\ -0.47\ \alpha'_2$
1426	$0.22\ \alpha_1\ -0.10\ \beta_2\ -0.19\ \alpha_2\ +0.09\ \beta_{10}$
1403	$0.18\ \alpha_1\ -0.09\ \beta_2\ +0.19\ \alpha_2\ -0.09\ \beta_{10}$
1381	$0.15\ \alpha'_1\ +0.15\ \alpha'_2\ +0.08\ \alpha'_3$
	$-0.14\ \beta'_1\ -0.14\ \beta'_2\ -0.14\ \beta'_3$
1314	$0.25\ Q'\ -0.17\ Q_4\ -0.09\ \beta_9\ +0.09\ \gamma_4$
1286	$0.31\ \beta_3\ -0.18\ \beta_4\ +0.12\ \beta_1\ +0.23\ Q_1$
1268	$0.42\ \beta_7\ -0.29\ \beta_8\ +0.12\ Q_3$
1159	$0.38\ Q_2\ +0.13\ \beta_4$
1036	$0.31\ \beta'_1\ -0.31\ \beta'_2\ +0.11\ \omega_5\ -0.15\ \omega_6$
1029	$0.14\ \beta_1\ -0.16\ \beta_2\ +0.11\ \beta_5\ -0.17\ \beta_6\ -0.12\ \beta'_3$
1000	$0.78\ \omega_2\ -0.11\ \tau_1$
996	$0.28\ \beta'_3\ +0.12\ Q_4$
985	$0.27\ \beta_9\ -0.31\ \beta_{10}\ +0.14\ \beta'_3$
909	$0.56\ \omega_1\ +0.10\ \omega_4\ +0.29\ \tau_1$
899	$0.58\ \omega_4\ -0.23\ \omega_1$
897	$0.66\ \omega_6\ +0.27\ \tau_5$
890	$0.26\ \beta_5\ -0.17\ \beta_6\ -0.16\ \beta_1\ +0.17\ \beta_2\ +0.15\ Q_2$
829	$0.61\ Q'\ +0.16\ Q_4$
740	$0.59\ \omega_3\ -0.12\ \omega_2\ -0.11\ \tau_1$
707	$0.53\ \tau_5\ +0.15\ \tau_1\ +0.11\ \omega_2$
611	$0.40\ \tau_1\ +0.27\ \omega_2$
530	$0.26\ \gamma_5\ -0.18\ \gamma_3\ +0.13\ \gamma_1\ -0.10\ \gamma_4$
512	$0.34\ \gamma_6\ -0.11\ \gamma_4\ +0.10\ \gamma_2$
478	$0.51\ \omega_5\ -0.10\ \omega_3\ -0.10\ \tau_3$
358	$0.20\ \gamma_1\ +0.18\ \gamma_4\ -0.13\ \gamma_6\ +0.09\ Q_2\ +0.08\ Q_3\ +0.11\ Q_4$
326	$0.21\ \gamma_5\ +0.18\ \gamma_2\ -0.15\ \gamma_1\ +0.10\ Q_4$
296	$0.39\ \tau_2\ -0.32\ \tau_4$
201	$0.81\ \chi$
166	$0.57\ \tau_3\ +0.10\ \omega_4\ +0.12\ \omega_5$
134	$0.33\ \gamma_3\ -0.26\ \gamma_2\ +0.10\ \gamma_1$
114	$0.33\ \tau_3\ -0.18\ \tau_2\ -0.15\ \tau_4\ +0.14\ \omega_3\ +0.13\ \omega_4$

le, the methyl group may be either staggered or eclipsed with respect to the neighbouring terminal hydrogen atom (H_7 for E2MH, H_6 for E3MH). For E2MH, the QCFF calculation led to an optimized geometry, where the in-plane methyl hydrogen is eclipsed with respect to the terminal hydrogen atom. This result agrees with expectations, since the interatomic distance is shorter between H'_3 and H_4 than between H'_3 and H_7 (after rotation by 180° of the methyl group), and this methyl conformation was used in our VFF calculations.

For E3MH, the interatomic distances H'_3–H_3 and H'_3–H_6 are nearly equal. Here, QCFF yielded an optimum geometry where the methyl hydrogens are staggered with respect to the terminal hydrogen atom, as shown in Fig. 5. However, QCFF geometry optimization starting with a terminal hydrogen-eclipsed geometry, led to non-planar structures with higher energies than for the planar, terminal hydrogen-staggered geometry. NMR experiments showed a conformation with the methyl hydrogens eclipsed with the terminal hydrogen atom to be predominant [29]. In the VFF calculations presented here, we used a methyl conformation with the methyl hydrogens staggered with the terminal hydrogen atom. We also carried out VFF calculations with the methyl hydrogens eclipsed with the terminal hydrogen atom, and these yielded vibrational frequencies that differed little from those presented in Tables 3 and 9.

Spectral assignments

It is clear from Tables 1–3 that the agreement between calculated and observed vibrational frequencies is far better for the VFF calculations than for the QCFF one. The QCFF frequencies are generally too high. QCFF is a semi-empirical method. *Ab initio* methods tend to over-estimate the force constants as well. Consequently, many *ab initio* calculations use "scaling factors" on the force constants [9, 20, 21, 43]. The experimental and calculated wavenumbers and assignments of the normal modes of E2MH, dE2MH and E3MH listed in Tables 1–6 are summarized together in Table 9, where only wavenumbers calculated by the VFF programs, not by the QCFF program, are listed.

Table 6. Calculated wavenumbers (cm^{-1}) and potential energy distributions of the normal modes of *E*-3-methyl-hexatriene in the region below 2000 cm^{-1}. Only the dominant contributions are shown. For notation, see Fig. 5

Wavenumber	Potential energy distribution
1637	$0.16\ Q_1 - 0.07\ Q_2 + 0.28\ Q_3 - 0.07\ Q_4 + 0.11\ Q_5$
1623	$0.26\ Q_1 - 0.32\ Q_5$
1583	$0.16\ Q_1 - 0.33\ Q_3 + 0.16\ Q_5$
1453	$0.66\ \alpha'_3 - 0.14\ \alpha'_1 - 0.14\ \alpha'_2$
1449	$0.47\ \alpha'_1 - 0.47\ \alpha'_2$
1429	$0.21\ \alpha_1 - 0.10\ \beta_2 - 0.19\ \alpha_2 + 0.09\ \beta_{10}$
1400	$0.17\ \alpha_1 - 0.08\ \beta_2 + 0.21\ \alpha_2 - 0.10\ \beta_{10}$
1382	$0.15\ \alpha'_1 + 0.15\ \alpha'_2 + 0.10\ \alpha'_3$
	$-0.14\ \beta'_1 - 0.14\ \beta'_2 - 0.17\ \beta'_3$
1340	$0.23\ Q' - 0.08\ Q_4 + 0.08\ \beta_5 - 0.19\ \beta_6$
1286	$0.35\ \beta_3 - 0.20\ \beta_4 + 0.12\ \beta_1 + 0.20\ Q_1$
1272	$0.19\ \beta_7 - 0.34\ \beta_8 - 0.12\ \beta_9 - 0.20\ Q_5$
1223	$0.26\ \beta_5 - 0.14\ \beta_6 + 0.05\ \beta_7$
	$+0.13\ Q_4 + 0.05\ Q_2 - 0.05\ Q' + 0.06\ \gamma_4$
1142	$0.34\ Q_2 - 0.10\ Q_4 + 0.11\ \beta_4 + 0.09\ \beta_1 - 0.07\ \beta_2$
1037	$0.19\ \beta_9 - 0.21\ \beta_{10} + 0.24\ \beta'_3$
1022	$0.35\ \beta'_1 - 0.35\ \beta'_2 + 0.12\ \omega_2$
996	$0.66\ \omega_5 - 0.15\ \omega_2 - 0.09\ \tau_5$
993	$0.45\ \omega_2 + 0.16\ \omega_5 - 0.11\ \tau_1$
980	$0.13\ \beta_9 - 0.13\ \beta_{10} + 0.08\ \beta_1 - 0.09\ \beta_2 - 0.16\ \beta'_3 + 0.12\ Q'$
936	$0.21\ \beta_1 - 0.24\ \beta_2 - 0.19\ Q_2$
908	$0.38\ \omega_1 - 0.35\ \omega_6 + 0.14\ \tau_1 - 0.12\ \tau_5$
906	$0.35\ \omega_1 + 0.37\ \omega_6 + 0.12\ \tau_1 + 0.14\ \tau_5$
812	$0.76\ \omega_3$
792	$0.53\ Q' + 0.18\ Q_4$
687	$0.40\ \tau_5 + 0.25\ \omega_5$
655	$0.51\ \tau_1 + 0.31\ \omega_2$
576	$0.24\ \gamma_5 - 0.20\ \gamma_6 + 0.08\ \gamma_2 - 0.08\ \gamma_4$
439	$0.26\ \gamma_4 - 0.20\ \gamma_3 + 0.11\ \gamma_1 - 0.12\ Q_4$
421	$0.41\ \omega_4 + 0.11\ \tau_2 - 0.13\ \tau_4$
360	$0.24\ \gamma_1 - 0.12\ \gamma_5 + 0.10\ Q_2 + 0.11\ Q_3$
291	$0.20\ \gamma_5 + 0.34\ \gamma_6$
275	$0.48\ \tau_3 + 0.17\ \tau_4 + 0.10\ \omega_4$
204	$0.43\ \tau_2 + 0.19\ \tau_3 - 0.11\ \omega_4 + 0.10\ \chi$
194	$0.81\ \chi + 0.11\ \tau_4$
158	$0.14\ \gamma_1 - 0.34\ \gamma_2 + 0.16\ \gamma_3$
126	$0.33\ \tau_3 - 0.21\ \tau_2 - 0.15\ \tau_4 + 0.17\ \omega_3$

For most of the vibrations in Table 9, the agreement between observed and calculated frequencies is good, even for the normal modes that are dominated by the strongly coupled CH rocks and C=C and C–C stretches. In particular, the VFF calculations are able to correctly predict the splitting of the C–C stretches for both E2MH and E3MH. The agreement again indicates the description of the normal modes found in Tables 4–6 to be reliable. However, there is some disagreement between observed and calculated frequencies for the in-plane rock of the methyl group (E3MH), for the in-plane skeletal deformations (E3MH), and for the low wavenumber torsions around the C–C bonds.

The force constants in Tables 7 and 8 that are related to the methyl group, were refined by us for isoprene, and for this compound the agreement between calculation and experiment was good. For isoprene, our calculated wavenumbers were 1036 cm^{-1} for the out-of-plane, and 992 cm^{-1} for the in-plane rock of the methyl group, whereas the observed values are 1034 [15] and 990 cm^{-1} [42], respectively.

In our VFF calculations for E2MH and dE2MH, the agreement between experiment and calculation is good for the methyl deformations around 1400 cm^{-1}, and for the in-plane methyl rock around 1010 cm^{-1}. The E2MH out-of-plane methyl rock may be assigned to the i.r. band at 1007 cm^{-1} or to the weak band at 1040 cm^{-1}. Only for the latter assignment does experiment and calculation (1038 cm^{-1}) agree.

For E3MH, our VFF calculations are in agreement with experiment for the methyl deformations and for the out-of-plane methyl rock, whereas the agreement is poor for the in-plane rock. The latter disagreement may be due to the interaction between the vibrations of the methyl group and those of the polyene chain being different for methylation in the 2- and 3-positions.

The in-plane skeletal C=C–C deformation at lowest wavenumber is unobserved for both E2MH, dE2MH and E3MH. For *E*-1,3,5-hexatriene, we have found a

b_u symmetry C=C–C deformation with medium i.r. intensity at 152 cm^{-1} [1]. In the present spectra of E2MH, dE2MH and E3MH, we observe the Raman $R(\bar{\nu})$ spectrum in the region below 400 cm^{-1}, not the far-i.r. spectrum. Consequently, a low wavenumber, mainly i.r. active vibration may very well be unobserved in the present study.

The agreement between calculation and experiment for the E3MH 456 and 392 cm^{-1} modes is not as good as for the corresponding modes in E2MH and dE2MH. However, the lowering of the E2MH 507 cm^{-1} mode, and the increase in the E2MH 372 cm^{-1} mode upon 3-methylation are predicted correctly.

After the above discussion of the imperfections in the description by the VFF calculations of the vibrational frequencies, attention should again be called to the fact that for most of the vibrations the agreement between calculation and experiment is fine. Moreover, although the vibrational patterns of E2MH, dE2MH and E3MH are quite different, the same force field is able to describe all three molecules, after changes in only three force constants, related to the central out-of-plane wags (see Table 8).

The vibrational patterns of E2MH, dE2MH and E3MH

Comparing Figs 1 and 3, the most notable difference between the Raman spectra of *E*-2-methyl-hexatriene and *E*-3-methyl-hexatriene is the high intensity of the E3MH 1226 cm^{-1} band. The ratio of the integrated intensities of the E3MH 1624 and 1226 cm^{-1} bands is *ca* 3. For the strongest bands of E2MH, at 1627 and 1166 cm^{-1}, the ratio is *ca* 5. The E2MH 1166 cm^{-1} band is described in Table 4 as C–C stretch, whereas the nature of the E3MH 1226 cm^{-1} band is described in Table 6 as CH rock, strongly coupled to C–C stretches. The E3MH 1145 cm^{-1} band, which is described in Table 6 as C–C stretch, is quite weak.

We have seen above that the observed spectra are reproduced satisfactorily by our VFF calculations. Consequently, it seems justified to build the following discussion of the vibrational patterns of E2MH, dE2MH and E3MH, not on the observed spectra in Tables 1–3, but on the spectra from the VFF calculations, as listed in Tables 4–6 and 9. The vibrational bands shall be referred to according to their frequencies as calculated by the VFF programs.

νC=C and sCH₂

For E2MH, the C=C stretching normal modes at 1644, 1626 and 1574 cm^{-1}, are centered on Q_5, Q_1 and Q_3, respectively. The same pattern is found for dE2MH, whereas for E3MH the C=C stretches resemble the + + +, +0−, and + − + combinations predicted by symmetry for unsubstituted *E*-1,3,5-hexatriene. For the 1637 cm^{-1} E3MH mode we note a + − + − + combination of the Q_1–Q_5 stretches. The CH_2 scissoring vibrations are symmetrical and similar for all three compounds, despite deuteriation and changes in methyl substitution.

dCH₃, wCH₃ and rCH₃

The methyl deformations around 1450 and 1380 cm^{-1} are highly localized in the methyl group, and they are similar for all three compounds investigated. For E2MH and dE2MH, the out-of-plane wag of the methyl group is coupled to the wag of H_7, for E3MH it is coupled to the wag of H_3. This difference may be related to the fact that the methyl group of E2MH is described as H_7-eclipsed, whereas that of E3MH is described as H_3-eclipsed. The in-plane methyl rock of E3MH is strongly coupled to the neighbouring CH_2 rock, more than for E2MH, and it is predicted at significantly higher wavenumbers than for E2MH and dE2MH. However, the observed frequency is even higher.

rCH₂

For E2MH, the CH_2 rock at 985 cm^{-1} is localized on C_6, and is barely changed upon deuteration, whereas the one at 949 cm^{-1} is localized on C_1. Deuteriation at H_4 lowers the H_4 rock, which then couples to the neighbouring 949 cm^{-1} (E2MH value) CH_2 rock, splitting it into 1029 and 890 cm^{-1} vibrations. Moving the methyl group from C_5 in E2MH to C_4 in E3MH, leaves the C_1-centered 949 cm^{-1} CH_2 rock nearly unaltered (E2MH 949, E3MH 936 cm^{-1}), whereas the CH_2 rock localized next to the methyl group is coupled to the in-plane rock of the methyl group through the $C_4C_7H'_3$ bend, and is split into 1037 and 980 cm^{-1} vibrations.

wCH₂

The pattern found above for the in-plane CH_2 rocks, localized in one end of the molecule, is also encountered for the out-of-plane CH_2 wags of E2MH and dE2MH. For E3MH, the 908 and 906 cm^{-1} modes are essentially C_{2h} symmetrical out-of-phase and in-phase combinations of the CH_2 wags centered on C_1 and C_6. As for the C=C stretches, the methyl substitution in E3MH gives rise to a smaller perturbation of the vibrations of C_{2h} symmetrical *E*-1,3,5-hexatriene.

wCH

For E2MH, the 1002 cm^{-1} vibration is described as a rather pure wag of H_3, whereas the wags of the two central hydrogen atoms are strongly coupled, giving rise to vibrations at 910 and 870 cm^{-1}. Deuteration of H_4 decouples the two central CH wags of dE2MH. For E3MH, we again encounter the symmetrical pattern, since the wags of H_3 and H_5 are coupled. A nearly pure wag of H_4 is found at 812 cm^{-1}, an unusually low wavenumber.

Skeletal modes

The C=C torsions are centered in order of decreasing frequency on τ_5, τ_1 and τ_3, for all three com-

Table 7. Non-zero force constants for *E*-2-methyl-hexatriene and 4-*d*-*E*-2-methyl-hexatriene. Units are mdyn/Å for diagonal stretch constants and stretch–stretch interactions, mdynÅ/rad^2 for diagonal bend or torsion constants and bend–bend interactions, and mdyn/rad for stretch–bend interactions

q_1q_1	5.479	q_1q_2	0.008	q_1Q_1	0.405	$q_1\alpha_1$	0.004	$q_1\beta_1$	0.224
q_2q_2	5.479	q_2q_3	0.068	q_2Q_1	0.405	$q_2\alpha_1$	0.004	$q_2\beta_2$	0.224
q_3q_3	5.470	q_3q_4	−0.024	q_3Q_1	0.395	q_3Q_2	0.370	$q_3\beta_3$	0.228
$q_3\beta_4$	0.215								
q_4q_4	5.470	q_4Q_2	0.370	q_4Q_3	0.395	$q_4\beta_5$	0.215	$q_4\beta_6$	0.228
q_4q_5	−0.024								
Q_1Q_1	8.320*	Q_1Q_2	0.230*	Q_1Q_3	−0.243*	$Q_1\beta_1$	0.254	$Q_1\beta_2$	0.254
$Q_1\gamma_1$	0.179	$Q_1\beta_3$	0.262	$Q_1\beta_5$	−0.036				
Q_2Q_2	4.640*	Q_2Q_3	0.230*	$Q_2\beta_1$	−0.036	$Q_2\gamma_1$	0.189	$Q_2\beta_4$	0.262
$Q_2\gamma_2$	0.189	$Q_2\beta_5$	0.262	Q_2Q_4	−0.126*	$Q_2\beta_7$	−0.036		
Q_3Q_3	7.650*	$Q_3\beta_4$	−0.036	$Q_3\gamma_2$	0.179	$Q_3\beta_6$	0.262	Q_3q_5	0.395
Q_3Q_5	−0.243*	Q_3Q_4	0.230*	$Q_3\gamma_4$	0.059†	$Q_3\gamma_5$	−0.059†	$Q_3\gamma_3$	0.179
$Q_3\beta_7$	0.262								
$\alpha_1\alpha_1$	0.436								
$\beta_1\beta_1$	0.581	$\beta_1\gamma_1$	0.026	$\beta_1\beta_3$	0.067				
$\beta_2\beta_2$	0.581	$\beta_2\gamma_1$	−0.028						
$\gamma_1\gamma_1$	0.778	$\gamma_1\gamma_2$	0.145	$\gamma_1\beta_5$	0.026				
$\beta_3\beta_3$	0.571*								
$\beta_4\beta_4$	0.571*	$\beta_4\gamma_2$	0.026	$\beta_4\beta_5$	0.067				
$\gamma_2\gamma_2$	0.980*	$\gamma_2\gamma_3$	0.145	$\gamma_2\beta_7$	0.026				
$\beta_5\beta_5$	0.557*								
$\beta_6\beta_6$	0.557*	β_6Q_4	−0.036	$\beta_6\gamma_3$	0.026	$\beta_6\beta_7$	0.067		
q_6q_6	5.479	q_6q_7	0.008	q_6Q_5	0.405	$q_6\alpha_2$	0.004	$q_6\beta_9$	0.224
q_7q_7	5.479	q_7Q_5	0.405	$q_7\alpha_2$	0.004	$q_7\beta_{10}$	0.224		
q_5q_5	5.470	q_5Q_4	0.370	$q_5\beta_8$	0.215	$q_5\beta_7$	0.228		
Q_5Q_5	8.320*	Q_5Q_4	0.230*	Q_5Q'	0.340‡	$Q_5\beta_9$	0.254	$q_5\beta_{10}$	0.254
$Q_5\gamma_4$	0.179	$Q_5\gamma_6$	0.179	$Q_5\gamma_3$	0.059†	$Q_5\beta_8$	−0.059†	$Q_5\beta'_1$	0.059†
$Q_5\beta'_2$	0.059†	$Q_5\beta'_3$	−0.059†						
Q_4Q_4	4.640*	Q_4Q'	0.340‡	$Q_4\beta_9$	−0.059†	$Q_4\beta_{10}$	0.059†	$Q_4\gamma_4$	0.189
$Q_4\gamma_5$	0.189	$Q_4\gamma_3$	0.189	$Q_4\beta_8$	0.262	$Q_4\beta'_1$	−0.059†	$Q_4\beta'_2$	−0.059†
$Q_4\beta'_3$	0.059†								
$Q'Q'$	4.160‡	$Q'\beta_9$	0.059†	$Q'\beta_{10}$	−0.059†	$Q'\gamma_6$	0.320§	$Q'\gamma_5$	0.320§
$Q'\gamma_3$	−0.059†	$Q'\beta_8$	0.059†	$Q'\beta'_1$	0.287§	$Q'\beta'_2$	0.287§	$Q'\beta'_3$	0.287§
$\alpha_2\alpha_2$	0.436								
$\beta_9\beta_9$	0.581	$\beta_9\gamma_4$	0.026	$\beta_9\gamma_6$	0.067†				
$\beta_{10}\beta_{10}$	0.581	$\beta_{10}\gamma_4$	0.067†	$\beta_{10}\gamma_6$	0.026				

$\gamma_4\gamma_4$	0.980*	$\gamma_4\gamma_3$	0.145	$\gamma_4\beta_8$	0.026				
$\gamma_6\gamma_6$	1.250‖	$\gamma_6\beta'_3$	−0.067†						
$\gamma_5\gamma_5$	1.250‖	$\gamma_5\gamma_3$	0.338†	$\gamma_5\beta_8$	0.067†	$\gamma_5\beta'_3$	0.067†		
$\gamma_3\gamma_3$	0.980*								
$\beta_8\beta_8$	0.557*								
$\beta_7\beta_7$	0.557*								
$q'_1q'_1$	5.064‡	$q'_1q'_2$	0.101‡	$q'_1q'_3$	0.101‡				
$q'_2q'_2$	5.064‡	$q'_2q'_3$	0.101‡						
$q'_3q'_3$	5.064‡								
$\alpha'_1\alpha'_1$	0.581‡	$\alpha'_1\alpha'_2$	−0.009†	$\alpha'_1\alpha'_3$	−0.009†				
$\alpha'_2\alpha'_2$	0.581‡	$\alpha'_2\alpha'_3$	−0.009†						
$\alpha'_3\alpha'_3$	0.581‡								
$\beta'_1\beta'_1$	0.673‡	$\beta'_1\beta'_2$	0.034†	$\beta'_1\omega_4$	0.018†	$\beta'_1\omega_5$	0.080†	$\beta'_1\omega_6$	0.018†
$\beta'_1\tau_4$	0.056†	$\beta'_1\tau_5$	−0.056†						
$\beta'_2\beta'_2$	0.673‡	$\beta'_2\omega_4$	−0.018†	$\beta'_2\omega_5$	−0.080†	$\beta'_2\omega_6$	−0.018†	$\beta'_2\tau_4$	−0.056†
$\beta'_2\tau_5$	0.056†								
$\beta'_3\beta'_3$	0.673‡								
$\omega_1\omega_1$	0.383	$\omega_1\omega_2$	0.198	$\omega_1\tau_1$	−0.292				
$\omega_2\omega_2$	0.497	$\omega_2\omega_3$	0.055¶	$\omega_2\tau_1$	−0.292	$\omega_2\tau_2$	0.116		
$\omega_3\omega_3$	0.435‖	$\omega_3\omega_4$	0.120‖	$\omega_3\tau_2$	0.116	$\omega_3\tau_3$	−0.301¶		
$\omega_4\omega_4$	0.435‖	$\omega_4\omega_5$	0.055¶	$\omega_4\tau_3$	−0.301¶	$\omega_4\tau_4$	0.116		
$\omega_5\omega_5$	0.589†	$\omega_5\omega_6$	0.198	$\omega_5\tau_4$	0.116	$\omega_5\tau_5$	−0.292	$\omega_5\chi$	0.030‡
$\omega_6\omega_6$	0.383	$\omega_6\tau_5$	−0.292						
$\tau_1\tau_1$	0.545	$\tau_1\tau_2$	0.011	$\tau_1\tau_3$	−0.017				
$\tau_2\tau_2$	0.261‖	$\tau_2\tau_3$	0.011						
$\tau_3\tau_3$	0.545¶	$\tau_3\tau_4$	0.011	$\tau_3\tau_5$	−0.017				
$\tau_4\tau_4$	0.297‖	$\tau_4\tau_5$	0.011						
$\tau_5\tau_5$	0.545								
$\chi\chi$	0.027‡								

Values not superscripted are from Ref [15], butadiene.
*Iterated by us for *E*-1,3,5-hexatriene.
†From Ref. [15], isoprene.
‡Iterated by us for isoprene.
§From Ref. [15], propene.
‖Iterated by us for *E*-2-methyl-hexatriene.
¶From Ref. [15], *E*-1,3,5-hexatriene.

Table 8. Non-zero force constants for *E*-3-methyl-hexatriene. Units are mdyn/Å for diagonal stretch constants and stretch–stretch interactions, mdyn Å/rad^2 for diagonal bend or torsion constants and bend–bend interactions, and mdyn/rad for stretch–bend interactions

q_1q_1	5.479	q_1q_2	0.008	q_1Q_1	0.405	$q_1\alpha_1$	0.004	$q_1\beta_1$	0.224
q_2q_2	5.479	q_2q_3	0.068	q_2Q_1	0.405	$q_2\alpha_1$	0.004	$q_2\beta_2$	0.224
q_3q_3	5.470	q_3q_4	−0.024	q_3Q_1	0.395	q_3Q_2	0.370	$q_3\beta_3$	0.228
$q_3\beta_4$	0.215								
q_4q_4	5.470	q_4Q_2	0.370	q_4Q_3	0.395	$q_4\beta_5$	0.215	$q_4\beta_6$	0.228
Q_1Q_1	8.320	Q_1Q_2	0.230	Q_1Q_3	−0.243	$Q_1\beta_1$	0.254	$Q_1\beta_2$	0.254
$Q_1\gamma_1$	0.179	$Q_1\beta_3$	0.262	$Q_1\beta_5$	−0.036				
Q_2Q_2	4.640	Q_2Q_3	0.230	$Q_2\beta_1$	−0.036	$Q_2\gamma_1$	0.189	$Q_2\beta_4$	0.262
$Q_2\gamma_2$	0.189	$Q_2\beta_5$	0.262	Q_2Q_4	−0.126	$Q_2\gamma_4$	−0.059		
Q_3Q_3	7.650	$Q_3\beta_4$	−0.036	$Q_3\gamma_2$	0.179	$Q_3\beta_6$	0.262	Q_3Q_5	−0.243
Q_3Q_4	0.230	Q_3Q'	0.340	$Q_3\gamma_6$	0.059	$Q_3\beta_7$	−0.036	$Q_3\gamma_3$	0.179
$Q_3\gamma_4$	0.179	$Q_3\beta'_1$	0.059	$Q_3\beta'_2$	0.059	$Q_3\beta'_3$	−0.059		
$\alpha_1\alpha_1$	0.436								
$\beta_1\beta_1$	0.581	$\beta_1\gamma_1$	0.026	$\beta_1\beta_3$	0.067				
$\beta_2\beta_2$	0.581	$\beta_2\gamma_1$	−0.028						
$\gamma_1\gamma_1$	0.778	$\gamma_1\gamma_2$	0.145	$\gamma_1\beta_5$	0.026				
$\beta_3\beta_3$	0.571								
$\beta_4\beta_4$	0.571	$\beta_4\gamma_2$	0.026	$\beta_4\beta_5$	0.067				
$\gamma_2\gamma_2$	0.980	$\gamma_2\gamma_3$	0.145	$\gamma_2\gamma_4$	0.338				
$\beta_5\beta_5$	0.557								
$\beta_6\beta_6$	0.557	β_6Q_4	−0.036	$\beta_6\gamma_3$	0.026	$\beta_6\gamma_4$	0.067		
q_6q_6	5.479	q_6q_7	0.008	q_6Q_5	0.405	$q_6\alpha_2$	0.004	$q_6\beta_9$	0.224
q_7q_7	5.479	q_7q_5	0.068	q_7Q_5	0.405	$q_7\alpha_2$	0.004	$q_7\beta_{10}$	0.224
q_5q_5	5.470	q_5Q_5	0.395	q_5Q_4	0.370	$q_5\beta_8$	0.228	$q_5\beta_7$	0.215
Q_5Q_5	8.320	Q_5Q_4	0.230	$Q_5\beta_9$	0.254	$Q_5\beta_{10}$	0.254	$Q_5\gamma_6$	0.179
$Q_5\beta_8$	0.262	$Q_5\gamma_3$	0.059	$Q_5\gamma_5$	−0.059				
Q_4Q_4	4.640	Q_4Q'	0.340	$Q_4\beta_9$	−0.036	$Q_4\gamma_6$	0.189	$Q_4\beta_7$	0.262
$Q_4\gamma_3$	0.189	$Q_4\gamma_5$	0.189	$Q_4\beta'_1$	−0.059	$Q_4\beta'_2$	−0.059	$Q_4\beta'_3$	0.059
$Q'Q'$	4.160	$Q'\gamma_6$	−0.059	$Q'\beta_7$	0.059	$Q'\gamma_5$	0.320	$Q'\gamma_4$	0.320
$Q'\beta'_1$	0.287	$Q'\beta'_2$	0.287	$Q'\beta'_3$	0.287				
$\alpha_2\alpha_2$	0.436								

$\beta_9\beta_9$	0.581	$\beta_9\gamma_6$	0.026	$\beta_9\beta_8$	0.067				
$\beta_{10}\beta_{10}$	0.581	$\beta_{10}\gamma_6$	−0.028						
$\gamma_6\gamma_6$	0.778	$\gamma_6\gamma_3$	0.145	$\gamma_6\gamma_5$	0.338				
$\beta_8\beta_8$	0.557								
$\beta_7\beta_7$	0.557	$\beta_7\gamma_3$	0.026	$\beta_7\gamma_5$	0.067				
$\gamma_3\gamma_3$	0.980								
$\gamma_5\gamma_5$	1.250	$\gamma_5\beta'_3$	0.067						
$\gamma_4\gamma_4$	1.250	$\gamma_4\beta'_3$	−0.067						
$q'_1q'_1$	5.064	$q'_1q'_2$	0.101	$q'_1q'_3$	0.101				
$q'_2q'_2$	5.064	$q'_2q'_3$	0.101						
$q'_3q'_3$	5.064								
$\alpha'_1\alpha'_1$	0.581	$\alpha'_1\alpha'_2$	−0.009	$\alpha'_1\alpha'_3$	−0.009				
$\alpha'_2\alpha'_2$	0.581	$\alpha'_2\alpha'_3$	−0.009						
$\alpha'_3\alpha'_3$	0.581								
$\beta'_1\beta'_1$	0.673	$\beta'_1\beta'_2$	0.034	$\beta'_1\omega_3$	0.018	$\beta'_1\omega_4$	0.080	$\beta'_1\omega_5$	0.018
$\beta'_1\tau_3$	−0.056	$\beta'_1\tau_4$	0.056						
$\beta'_2\beta'_2$	0.673	$\beta'_2\omega_3$	−0.018	$\beta'_2\omega_4$	−0.080	$\beta'_2\omega_5$	−0.018	$\beta'_2\tau_3$	0.056
$\beta'_2\tau_4$	−0.056								
$\beta'_3\beta'_3$	0.673								
$\omega_1\omega_1$	0.383	$\omega_1\omega_2$	0.198	$\omega_1\tau_1$	−0.292				
$\omega_2\omega_2$	0.497	$\omega_2\omega_3$	0.055	$\omega_2\tau_1$	−0.292	$\omega_2\tau_2$	0.116		
$\omega_3\omega_3$	0.405*	$\omega_3\omega_4$	0.196*	$\omega_3\tau_2$	0.116	$\omega_3\tau_3$	−0.301		
$\omega_4\omega_4$	0.557*	$\omega_4\omega_5$	0.055	$\omega_4\tau_3$	−0.301	$\omega_4\tau_4$	0.116	$\omega_4\chi$	0.030
$\omega_5\omega_5$	0.497	$\omega_5\omega_6$	0.198	$\omega_5\tau_4$	0.116	$\omega_5\tau_5$	−0.292		
$\omega_6\omega_6$	0.383	$\omega_6\tau_5$	−0.292						
$\tau_1\tau_1$	0.545	$\tau_1\tau_2$	0.011	$\tau_1\tau_3$	−0.017				
$\tau_2\tau_2$	0.261	$\tau_2\tau_3$	0.011						
$\tau_3\tau_3$	0.545	$\tau_3\tau_4$	0.011	$\tau_3\tau_5$	−0.017				
$\tau_4\tau_4$	0.297	$\tau_4\tau_5$	0.011						
$\tau_5\tau_5$	0.545								
$\chi\chi$	0.027								

Values not superscripted are transferred from Table 7.
*Iterated by us for *E*-3-methyl-hexatriene.

Table 9. Symmetry, observed (mostly Raman values) and calculated (VFF) wavenumbers (cm^{-1}), and approximate description of normal modes of vibration of *E*-2-methyl-hexatriene (E2MH), 4-*d*-*E*-2-methyl-hexatriene (dE2MH), and *E*-3-methyl-hexatriene (E3MH)

	a'						*a''*					
	E2MH		dE2MH		E3MH		E2MH		dE2MH		E3MH	
	obs	calc	obs	calc	obs	calc	obs	calc	obs	calc	obs	calc
*d*CH	1455	1453	1450	1453	1459	1453	1440	1449	1439	1449	1443	1449
	1374	1381	1376	1381	1387	1382						
rCH_3	1019	1008	1011	996	1067	1037						
wCH_3							1040	1038	—	1036	1034	1022
sCH_2	1415	1428	1413	1426	1424	1429						
	1398	1403	1393	1403	1402	1400						
rCH_2	988	985	980	985	985	980						
	947	949	1039	1029	946	936						
wCH_2							894	908	907	909	906	908
							888	897	897	897	901	906
*r*CH	1301	1287	1292	1286	1298	1286						
	1288	1284	1274	1268	1257	1272						
	1257	1251	884	890	1226	1223						
*w*CH							1002	1002	992	1000	990	996
							900	910	900	899	984	993
							865	870	768	740	803	812
Skeleton												
*v*C=C	1631	1644	1628	1644	1624	1637						
	1627	1626	1615	1620	1620	1623						
	1585	1574	1578	1563	1577	1583						
*v*C–C	1316	1320	1311	1314	1348	1340						
	1166	1162	1159	1159	1145	1142						
	843	829	839	829	788	792						
*d*CCC	540	549	515	530	584	576						
	507	513	506	512	456	439						
	372	358	370	358	392	360						
	325	330	320	326	301	291						
	—	134	—	134	—	158						
*t*C=C							705	707	707	707	685	687
							634	633	612	611	648	655
							186	174	169	166	256	275
wCH_3							493	484	485	478	420	421
rotCH_3							229	202	225	201	181	194
*t*C–C							—	309	—	296	—	204
							146	114	143	114	156	126

pounds. The CC torsion at lowest frequency is a $-+-$ combination of the τ_2, τ_3 and τ_4 torsions for all three compounds. The 309 cm^{-1} vibration of E2MH and the 296 cm^{-1} vibration of dE2MH are combinations of the τ_2 and τ_4 torsions, whereas the 204 cm^{-1} vibration of E3MH is centered on τ_2. This is in contrast to the above, where E3MH has shown the most symmetrical vibrations, and indicates that the methyl substituent on C_4 decouples the C–C torsions.

The skeletal methyl wag and, especially, the torsion of the methyl group couple little to other vibrations for all three compounds. Because of the crowded environment of the methyl hydrogens in E3MH, the barrier to methyl rotation should be lower than for E2MH. This indeed seems to be the case, since the methyl rotation is observed experimentally at 229 cm^{-1} for E2MH, at 225 cm^{-1} for dE2MH, and at 181 cm^{-1} for E3MH.

*ν*C–C *and r*CH

For *E*-1,3,5-hexatriene, the two in-chain C–C stretches couple, and lead to an in-phase combination at 1188 cm^{-1} and an out-of-phase combination at 1132 cm^{-1} [1]. For isoprene, the two C–C stretches (one in-chain and one lateral) couple strongly, and give rise to an out-of-phase combination at 1303 cm^{-1} and an in-phase combination at 778 cm^{-1} [15]. The same pattern as for isoprene is encountered for lateral methylation in *E*-2,5-dimethyl-1,3,5-hexatriene [1].

For isoprene, *E*-2,5-dimethyl-hexatriene and E2MH, the methyl groups are substituted on terminal C=C bonds, whereas for E3MH the methyl group is substituted on the central C=C bond. Hence, we expect isoprene, *E*-2,5-dimethyl-hexatriene and E2MH to resemble each other with respect to coupling between CC stretches, whereas E3MH may be different.

For E2MH, one might envisage two situations. If the two ends of the molecule interact little, one would expect to find bands corresponding to the *E*-hexatriene case and bands that correspond to the *E*-2,5-dimethyl-hexatriene situation. If the two ends interact strongly, one would expect an intermediate situation. Actually, we find for E2MH, one normal mode that is close to those of *E*-hexatriene and two that correspond to *E*-2,5-dimethyl-hexatriene normal modes. Thus it seems that the chain C–C stretch, which has no atom in common with the C-methyl stretch, is coupled little to the other C–C stretches, so the two ends of the molecule interact little with respect to coupling between C–C stretching vibrations. Comparing E2MH and E3MH, we can also follow how the coupling of the C–C stretches with the CH rocks is altered with the position of the methyl group. We shall now discuss these effects more precisely.

For E2MH, the three CH rocks are centered on H_3, H_5 and H_4, in order of decreasing wavenumber, and are coupled to each other and to C=C and C–C stretches. The Q_2 stretch couples to the neighbouring CH_2 and H_3 rocks, whereas the Q_4 and Q' stretches couple and split into out-of-phase 1320 and in-phase 829 cm^{-1} combinations. Deuteration at H_4 does not change this pattern for E2MH much, except for the H_4 rock, which is decoupled from the H_5 rock and lowered to a frequency where it can couple to the $C_1H_1H_2$ rock, leading to vibrational modes at 1029 and 890 cm^{-1}. Although 890 cm^{-1} corresponds to a decrease by a factor of $\sqrt{2}$ of 1251 cm^{-1} (the frequency of the H_4 rock in E2MH), there is a substantial H_4 rock contribution to both the 1029 and 890 cm^{-1} modes.

For E2MH, we thus find that the Q_4 and Q' stretches couple in the same way as for isoprene, whereas the Q_2 stretch couples little to the other C–C stretches, and is found at a frequency (1166 cm^{-1} experimentally) close to the average of the 1188 and 1132 cm^{-1} C–C stretches of *E*-1,3,5-hexatriene.

We now go on to E3MH. The vibrational pattern of E3MH is more complicated, with stronger coupling between C–C stretches and CH rocks, as reflected in the presence of two bands in the observed spectra, at 1413 and 1323 cm^{-1}, that cannot be assigned to fundamentals. We shall now assign these two bands.

With its high intensity, the experimental 1413 cm^{-1} band is likely to be a Fermi resonance. The experimental 420 cm^{-1} band, combined with the experimental 990 cm^{-1} band (or with the 984 cm^{-1} band), gives rise to a 1410 (or 1404) cm^{-1} combination of a' symmetry. This 1410 (or 1404) cm^{-1} combination may be in Fermi resonance with the 1402 cm^{-1} band of a' symmetry. The 1323 cm^{-1} band is likely to represent a combination, probably between the 420 cm^{-1} methyl wag and one or both of the 906 and 901 cm^{-1} CH_2 wags.

Turning now to the C–C stretches of E3MH, these may be viewed in two different ways. In the first view, the C–C stretches of E3MH may be described as for E2MH and dE2MH, with the out-of-phase combination of the Q_4 and Q' stretches at 1340 cm^{-1}, the in-phase combination at 792 cm^{-1}, and the Q_2 stretch at 1142 cm^{-1}.

Alternatively, in the second view one may speak of hexatriene-like and isoprene-like combinations of the C–C stretches, that again couple to each other. The Q_2 and Q_4 stretches couple hexatriene-like, leading to a Q_2+Q_4 combination around 1188 cm^{-1} and a Q_2-Q_4 combination around 1132 cm^{-1}. The Q_4 and Q' stretches couple isoprene-like, leading to a Q_4-Q' combination around 1303 cm^{-1} and a Q_4+Q' combination around 778 cm^{-1}. The two lowest of these vibrations (Q_4+Q' and Q_2-Q_4) are sufficiently isolated in frequency and so do not couple further. Their calculated frequencies (792 and 1142 cm^{-1}) support this picture.

Q_4-Q' and Q_2+Q_4 couple with each other and with the H_4 rock. The calculated 1223 cm^{-1} mode thus contains both Q_2+Q_4 and Q_4-Q' character, though it is dominated by the H_4 rock. The calculated 1340 cm^{-1} mode contains H_4 rock, but is dominated by Q_4-Q'. With the appearance of modes with Q_2

$+Q_4$ and Q_2-Q_4 character, we again see a resemblance between E3MH and E-1,3,5-hexatriene.

The fact that the coupling between Q' stretch and H_4 rock in E3MH is stronger than the coupling in E2MH between Q' stretch and H_5 rock (and the coupling in E3MH between Q' stretch and H_5 rock) is in agreement with expectations, since vibrational coupling is usually stronger through a C=C double bond than through a C–C single bond.

The character found in the present study for the C–C stretching modes of E2MH is in agreement with our interpretation of the C–C stretching modes of E-2,5-dimethyl-hexatriene in Ref. [1]. The coupling between chain and lateral C–C stretches has been observed previously for methylated derivatives of butadiene [15, 44], and has been termed a νCC_2 stretch.

We have here found that in E2MH the Q_4+Q' and Q_4-Q' combinations couple little with the Q_2 stretch. Moreover, we have found that for E3MH the Q_2 stretch is not isolated, since the Q_4 stretch couples with both the Q' stretch and the Q_2 stretch. This result is important, since E3MH is an appropriate model for the longer polyenes like retinal and β-carotene, where the methyl groups are substituted on internal C=C bonds, as in E3MH.

CONCLUSIONS

In the present paper we have obtained the vibrational spectra of E-2-methyl-hexatriene, 4-d-E-2-methyl-hexatriene, and E-3-methyl-hexatriene. The spectra are interpreted using semi-empirical QCFF/π calculations and empirical valence force field calculations. For QCFF/π the agreement with experiment was unsatisfactory. The empirical valence force fields of the three compounds were iterated on the basis of valence force fields of butadiene, isoprene and E-hexatriene, and the agreement of final calculated frequencies with experimental ones was fine. Consequently, our discussion of the molecular vibrations is based on the calculations using empirical valence force fields.

We have found that many normal modes of E-hexatriene are changed less by 3-methylation than by 2-methylation. Methylation in the 2-position seems to perturb the C_{2h} symmetry of E-hexatriene more than does 3-methylation.

A distinction is made in Ref. [38] between unsubstituted polyenes with global symmetry coordinates, and retinal with local symmetry coordinates. The fact that the vibrations of E-3-methyl-hexatriene are more similar to the vibrations of E-hexatriene than are the vibrations of E-2-methyl-hexatriene indicates a modification of this distinction, since the position of the substitution also determines the degree to which the symmetry coordinates can be characterized as global or local. In this respect, the local symmetry of the methyl groups of the all-*trans* isomers of retinal and β-carotene rather corresponds to E-3-methyl-hexatriene than to E-2-methyl-hexatriene.

The coupling between chain C–C and C–methyl stretches takes place in both E-2-methyl-hexatriene and E-3-methyl-hexatriene. However, coupling between these C–C stretch combinations and the isolated C–C stretch is found only for E-3-methyl-hexatriene, where combinations of the chain C–C stretches similar to those of E-hexatriene are present and couple to the C-methyl stretch.

We also find that coupling between the chain C–C and C–methyl stretch combination and neighbouring CH rock is stronger through a C=C bond (E-3-methyl-hexatriene) than through a C–C bond (E-2-methyl-hexatriene). This result agrees with expectation.

On the basis of the QCFF/π calculation we assume the methyl group of E-2-methyl-hexatriene to be eclipsed, and the E-3-methyl-hexatriene methyl group to be staggered with respect to the neighbouring CH_2 group. Greater steric hindrance in the most stable rotamer implies that the barrier to rotation of the methyl group must be lower for E-3-methyl-hexatriene than for E-2-methyl-hexatriene. This is qualitatively confirmed by a study of relaxation rates in ^{1}H NMR.

The methyl deformations are highly localized in the methyl group. The in-plane rocks and out-of-plane wags of the methyl group are strongly coupled to neighbouring CH and CH_2 in-plane rocks and out-of-plane wags, respectively. The differences between E-2-methyl-hexatriene and E-3-methyl-hexatriene in these couplings can be explained by the differences in methyl conformation mentioned above, and the differences in the barrier to methyl rotation is reflected in the frequencies of the methyl rotation.

Acknowledgements—The authors wish to thank Drs O. F. NIELSEN, F. M. NICOLAISEN and G. O. SØRENSEN, Chemical Laboratory V, H. C. Ørsted Institute, University of Copenhagen, for help with spectra and VFF calculations, and Dr R. J. A. GRIM, Astrophysics Group, Huygens Laboratory, Leiden, for help in obtaining the i.r. spectrum of matrix-isolated E2MH. The Danish Natural Science Research Council is gratefully acknowledged for a grant to F.W.L. (Grant No. 11-6151), and for a grant to purchase the Bruker FT-i.r. spectrometer (Grant No. 11-3832). This work was supported by a collaborative research grant from NATO (Grant No. 0137/88).

REFERENCES

[1] F. W. LANGKILDE, R. WILBRANDT, O. F. NIELSEN, D. H. CHRISTENSEN and F. M. NICOLAISEN, *Spectrochim. Acta* **43A**, 1209 (1987).
[2] E. R. LIPPINCOTT, C. E. WHITE and J. P. SIBILIA, *J. Am. chem. Soc.* **80**, 2926 (1958).
[3] E. R. LIPPINCOTT and T. E. KENNEY, *J. Am. chem. Soc.* **84**, 3641 (1962).
[4] R. M. GAVIN JR and S. A. RICE, *J. chem. Phys.* **55**, 2675 (1971).
[5] Y. N. PANCHENKO, Y. A. PENTIN and E. B. RUSACH, *Russ. J. phys. Chem.* **49**, 1536 (1975).
[6] Y. N. PANCHENKO and E. B. RUSACH, *Chem. Bull., Moscow State Univ.* **20**, 221 (1979).
[7] D. RAKOVIC, S. A. STEPANYAN, L. A. GRIBOV and Y. N. PANCHENKO, *J. molec. Struct.* **90**, 363 (1982).

[8] Y. N. PANCHENKO, P. CSÁSZÁR and F. TÖRÖK, *Acta chim. hung.* **113**, 149 (1983).
[9] C. W. BOCK, Y. N. PANCHENKO, S. V. KRASNOSHCHIOKOV and V. I. PUPYSHEV, *J. molec. Struct.* **148**, 131 (1986).
[10] A. C. LASAGA, R. J. AERNI and M. KARPLUS, *J. chem. Phys.* **73**, 5230 (1980).
[11] B. S. HUDSON, B. E. KOHLER and K. SCHULTEN, in *Excited States*, Vol. 6, pp. 1–95 (edited by E. C. LIM). Academic Press, New York (1982).
[12] D. G. LEOPOLD, R. D. PENDLEY, J. L. ROEBBER, R. J. HEMLEY and V. VAIDA, *J. chem. Phys.* **81**, 4218 (1984).
[13] R. J. HEMLEY, B. R. BROOKS and M. KARPLUS, *J. chem. Phys.* **85**, 6550 (1986).
[14] A. B. MYERS, R. A. MATHIES, D. J. TANNOR and E. J. HELLER, *J. chem. Phys.* **77**, 3857 (1982).
[15] B. CURRY, Ph.D. Thesis, University of California, Berkeley (1983).
[16] J. A. HERBIG, Dissertation, Universität zu Köln (1964).
[17] S. J. CYVIN, G. HAGEN and M. TRÆTTEBERG, *Acta chem. scand.* **23**, 3285 (1969).
[18] Y. FURUKAWA, H. TAKEUCHI, I. HARADA and M. TASUMI, *J. molec. Struct.* **100**, 341 (1983).
[19] R. MCDIARMID and A. SABLJIC, *J. phys. Chem.* **91**, 276 (1987).
[20] P. G. SZALAY, A. KARPFEN and H. LISCHKA, *J. chem. Phys.* **87**, 3530 (1987).
[21] G. FOGARASI, P. G. SZALAY, P. P. LIESCHESKI, J. E. BOGGS and P. PULAY, *J. molec. Struct.* **151** 341 (1987).
[22] F. W. LANGKILDE, Doctoral Dissertation, Risø-M-2644, Risø (1987).
[23] F. W. LANGKILDE, R. WILBRANDT and N.-H. JENSEN, *Chem. phys. Lett.* **111**, 372 (1984).
[24] F. W. LANGKILDE, N.-H. JENSEN and R. WILBRANDT, *Chem. phys. Lett.* **118**, (1985) 486.
[25] F. W. LANGKILDE, N.-H. JENSEN and R. WILBRANDT, *Springer Proc. Phys.* **4**, 175 (1985).
[26] F. W. LANGKILDE, N.-H. JENSEN, R. WILBRANDT, A. M. BROUWER and H. J. C. JACOBS, *J. phys. Chem.* **91**, 1029 (1987).
[27] F. W. LANGKILDE, N.-H. JENSEN and R. WILBRANDT, *J. phys. Chem.* **91**, 1040 (1987).
[28] J. C. W. CHIEN, *Polyacetylene, Chemistry, Physics and Material Science*. Academic Press, Orlando, FL (1984).
[29] A. M. BROUWER, Ph.D. Thesis, Leiden, Netherlands (1987).
[30] A. M. BROUWER and H. J. C. JACOBS, to be published.
[31] W. HAGEN, L. J. ALLAMANDOLA and J. M. GREENBERG, *Astrophys. Space Sci.* **65**, 215 (1979).
[32] S. BJØRKLUND, E. AUGDAHL, D. H. CHRISTENSEN and G. O. SØRENSEN, *Spectrochim. Acta* **32A**, 1021 (1976).
[33] A. WARSHEL and M. KARPLUS, *J. Am. chem. Soc.* **94**, 5612 (1972).
[34] A. WARSHEL and M. LEVITT, *Quantum Chem. Progm Exch.* **11**, 247 (1974).
[35] O. F. NIELSEN, P.-A. LUND and E. PRÆSTGAARD, *J. chem. Phys.* **77**, 3878 (1982).
[36] L. M. SVERDLOV, M. A. KOVNER and E. P. KRAINOV, *Vibrational Spectra of Polyatomic Molecules*. Wiley, New York (1974).
[37] M. RYTEL, *Opt. Spectrosc.* **16**, 402 (1964).
[38] B. CURRY, I. PALINGS, A. D. BROEK, J. A. PARDOEN, J. LUGTENBURG and R. MATHIES, in *Advances in Infrared and Raman Spectroscopy*, Vol. 12, pp. 115–178 (edited by R. J. H. CLARK and R. E. HESTER). Wiley Heyden (1985).
[39] M. TRÆTTEBERG and G. PAULEN, *Acta chem. scand.* **A28**, 1150 (1974).
[40] C. W. BOCK, Y. N. PANCHENKO, S. V. KRASNOSHCHIOKOV and R. AROCA, *J. molec. Struct.* **160**, 337 (1987).
[41] F. INAGAKI, M. TASUMI and T. MIYAZAWA, *J. Raman Spectrosc.* **3**, 335 (1975).
[42] D. A. C. COMPTON, W. O. GEORGE and W. F. MADDAMS, *J. chem. Soc. Perkin II* 1666 (1976).
[43] P. PULAY, G. FOGARASI, G. PONGOR, J. E. BOGGS and A. VARGHA, *J. Am. chem. Soc.* **105**, 7037 (1983).
[44] M. M. ABO ALY, M. H. BARON, M. J. COULANGE and J. FAVROT, *Spectrochim. Acta* **42A**, 411 (1986).